Active Clamp Dual Flyback Inverter for Low Cost and High-Efficient Microinverter Application

FRIVALDSKY, M.
Department of mechatronics and electronics
University of Zilina
Univerzitna 1, 010 26, Zilina
SLOVAKIA
Michal.frivaldsky@fel.uniza.sk

Abstract: - The paper deals with the analysis and experimental verification of dual fly-back SiC inverter (DFBI) suited for isolated, low cost and high-efficiency photovoltaic microinverter application, while active and reactive power generation is possible. The DFBI topology is relatively simple single stage DC/AC power conversion topology. High power conversion efficiency can be reached with this topology if modern SiC devices and active clamp, quasi-resonant switching circuitry are implemented within DFBI design. The state-space analysis makes possible to work-out DC transfer characteristics depending on duty cycle control parameter, whereby this dependency is consequently implemented within the experimental sample. Efficiency characteristics of DFBI inverter are investigated at different switching frequencies and circuit parameters in order to better understand the technical limits of this power topology.

Key-Words: - microinverter, high-efficiency, bidirectional, quasi-resonant

1 Introduction

Dual fly-back inverter (DFBI) is one of the preferred topologies for isolated low power low cost photovoltaic (PV) inverters [1]. It can be used for grid-connected power systems or for island operation power systems. Both active and reactive power can be generated by DFBI inverter while keeping reduced component count. Island operation requires high-performance output voltage control algorithm which will ensure that output AC voltage will remain quasi-harmonic and within operating limits under the different load and input voltage conditions [2].

Nowadays, the main focus within PV systems is continuously given on the system´s efficiency increase. For these purposes, various techniques can be utilized, e.g. research and application of new concepts of power converter topologies [3], [4] and development of novel control algorithms [5], [6].

Even these methods are valuable, they may have a disadvantage from a complexity point of view. Rather than that, there exist also scientific procedures, which are based on the investigation of well-known and practically verified solutions, whereby impact is given on the research of possibilities of new materials utilization (e.g. new semiconductor materials, new magnetic materials etc…). Thus the different operational condition of existing and improved solutions can be investigated (change of switching frequency or use of improved clamping control) [7] - [14].

Almost due to previous facts, in this paper, we are showing theoretical analysis and experimental verification of improved dual-flyback inverter (DFBI) suited for low-cost, high efficient PV microinverter applications.

2 Theoretical analysis

Given theoretical analysis serves to a better understanding of DFBI operation, for determination of the duty cycle within open-loop steady state operation, and for DC voltage transfer characteristics derivation, while it is then used for the determination of critical duty cycle due to its non-linear character. A sinusoidal harmonic voltage has to be generated in grid network island operation. DFBI inverter functionality can be easily explained using boost type inverter which is shown on Fig.1.

Let's assume that control circuit (by means of duty cycle control of switches S1, S2, S3, S4) can generate following voltages across C1 and C2 capacitors:

$$u_{C1}(t) = U_{DC} + \frac{1}{2}U_{max}\cos(2 \quad _{ůb}t) \tag{1}$$

$$u_{C2}(t) = U_{DC} - \frac{1}{2}U_{max}\cos(2 \quad _{ůb}t) \tag{2}$$

U_{DC} is DC offset voltage (u_{C1}, u_{C2} voltages have positive polarity only) and U_{max} is required amplitude of AC voltage. The DC offset voltage needs to be set properly to prevent uncontrolled charging of C_1, C_2 capacitors from input power source. It is obvious that output AC voltage is subtraction of C_1, C_2 capacitors voltages:

$$u_{AC}(t) = u_{C1}(t) - u_{C2}(t) = U_{max}\cos(2\ \hat{u}_b t) \quad (3)$$

$$\cos^2(\omega_b t) = \frac{1+\cos(2\omega_b t)}{2} \text{ and } \sin^2(\omega_b t) = \frac{1-\cos(2\omega_b t)}{2} \quad (4\,a,b)$$

By subtraction of (4a) – (4b) we obtain relationships between cosine and sine functions, respectively:

$$\cos^2(\omega_b t) - \sin^2(\omega_b t) = \cos(2\omega_b t) \text{ or } \cos(\ \hat{u}_b t) = \cos^2\left(\frac{\hat{u}_b}{2} t\right) - \sin^2\left(\frac{\hat{u}_b}{2} t\right) \quad (5a,b)$$

So, by such a way (5 a,b), the output voltage U_{out} of the inverter can be a sinusoidal harmonic function.

Output voltage u_{AC} becomes harmonic without any DC offset. DFBI inverter is derived from boost inverter by replacing L_1, L_2 inductors with fly-back transformers (fig. 1). This will cause that input and output of DFBI inverter will be galvanically isolated what prevents safety-related issues in PV systems.

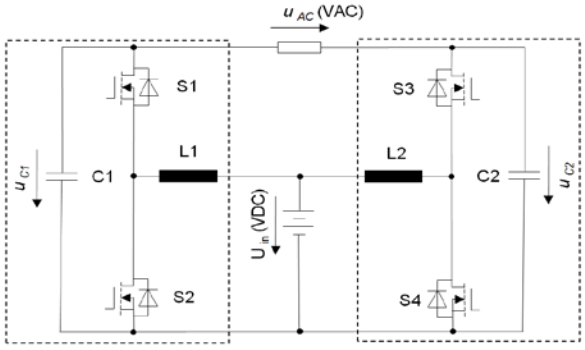

Figure 1. *Buck-boost bidirectional flyback replacement of the DFBI inverter considering parasitic resistance*

The proposed converter is based on the principal topology, whose schematic is shown in Fig. 2. This converter can be classified as DC-DC buck-boost fly-back converter. The following analysis is oriented on the determination of state space variables and on the investigation of the voltage-transfer characteristic in both direct and recuperative mode of operation. The operation of converter for both directions of power flow (energy transfer from the power source into load and energy recuperation from load into a power source) can be divided into two operating intervals:

- interval $t \in \langle t_0 - t_s \rangle$: transistor T_1 (T_2) closed, transistor T_2 (T_1) open;
- interval $t \in \langle t_s - T \rangle$: transistor T_1 (T_2) open, transistor T_2 (T_1) closed.

3 Control system requirement

The control system provides a harmonic waveform for the output voltage given by Eqs. (1)-(2). So, each fly-back output voltage must follow $\sin^2(\omega t)$ or $\cos^2(\omega t)$ waveforms by means of duty cycle control. So, using (1b) yields:

$$u_{ref}(t) = U_{max}\left[\frac{1}{2} - \frac{\cos(2\ \hat{u}_b t)}{2}\right] \quad (9)$$

where:

U_{max} - maximal voltage corresponding to demanded one which can be determined from voltage DC transfer characteristic of the modified fly-back converter [15] (Fig. 2).

From fig. 2 can be seen that if we demand output voltage for two multiple of V_{in} the corresponding duty cycle D is 0.75.

Note: the critical value of duty cycle D_{crit} (~0.85) under nominal load cannot be exceeded.

Pumped energy (PE) [16] during switching period (T):

$$PE = \Delta W_L = W_L(t_s) - W_L(0) = \frac{1}{2}LI_L^2(t_s) - \frac{1}{2}LI_L^2(0) = \frac{1}{2}L\left[I_L^2(t_s) - I_L^2(0)\right] \quad (10)$$

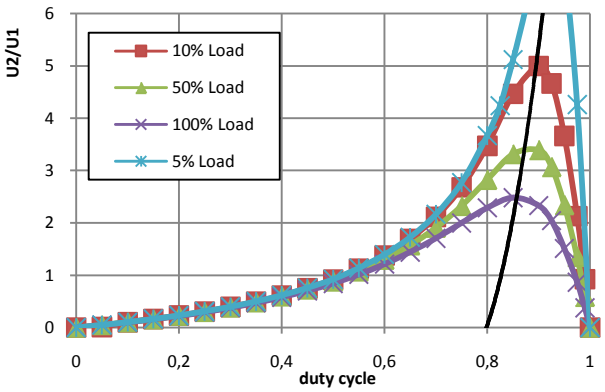

Figure 2. *Voltage DC transfer characteristic of modified buck-boost bidirectional flyback replacement under various load 0% - 100% P_{OUT}*

The decline of capacitor energy during energy pumping:

$$-\Delta W_C = W_C(0) - W_C(t_s) = \frac{1}{2}LI_L^2(T) - \frac{1}{2}LI_L^2(t_s) = \frac{1}{2}L\left[I_L^2(T) - I_L^2(t_s)\right] \quad (11)$$

The decline of inductor energy transferred to secondary circuit during this process, i.e. decline of inductor energy:

$$-\Delta W_L = W_L(T) - W_L(t_s) = \frac{1}{2}LI_L^2(T) - \frac{1}{2}LI_L^2(t_s) = \frac{1}{2}L\left[I_L^2(T) - I_L^2(t_s)\right] \quad (12)$$

Referenced capacitor voltage average value during energy pumping is:

$$U_{Cref} = \frac{1}{T_b}\int_0^T u_{Cref}(t)dt = \frac{1}{T_b}\int_0^T U_{max}\sin^2(\omega_b t)dt \quad (13)$$

, where

T_b is a time period of basic harmonic.

Then demanded capacitor energy is:

$$W_C = \frac{1}{2}CU_{Cref}^2(T) \quad (14)$$

Stored energy (SE) during the switching period (T):

$$SE = \Delta W_{LC} = \Delta W_L + \Delta W_C \quad (15)$$

Total stored energy (SE) on the end of the switching period (T):

$$SE(T) = W_{LC} = W_L(T) + W_C(T) \quad (16)$$

So active energy and energy losses yields:

$$EL = P_{T-s}.T = (P_2 + P_{loss})\,T \quad (17)$$

We can define power losses as the resistance power lossesP_r passive element power losses P_e and device power losses P_d. The total power losses P_{loss} are the sum of them. Then:

$$\Delta W_L = \Delta W_C + EL, \quad (18)$$

For energy balancing is necessary to take into account that $u_C(T)$ should be equal to reference value:

$$u_C(T) = u_{Cref}(T). \quad (19)$$

4 Efficiency determination

The principal dependency of efficiency on duty cycle is shown in Fig. 3, which was derived based on a steady-state calculation of Eqs. (3) - (5).

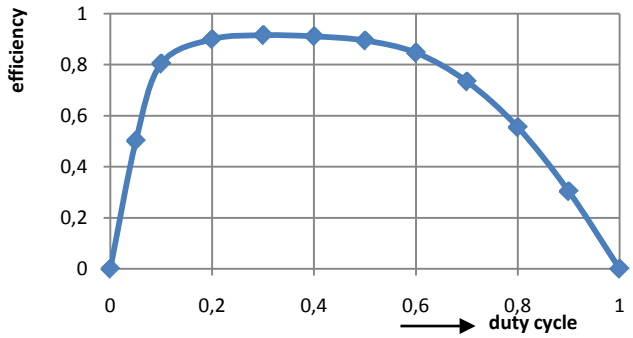

Figure 3. *The calculated dependence of efficiency on duty cycle at 30 Vdc of the input voltage and 200 W of output power.*

Regarding efficiency optimization and taking into account dependencies in fig.3, it is possible to optimize the range of duty cycle under nominal load from 0,2 to 0,6 respectively.

5 Experimental verification of DFBI performance

Extensive computer simulation analysis of DFBI inverter was performed in [7], [9] and [12]. The simulation was focused on efficiency analysis of DFBI inverter with the use of novel switching devices (including SiC components). It was found out that secondary rectification done by switch S3 (fig. 5) is most important for the high-efficiency operation of this power topology.

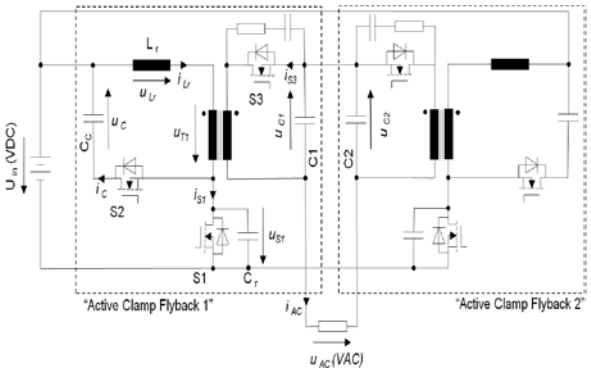

Figure 4. *Principal schematic of active clamp DFBI inverter for experimental analysis*

The experimental results are shown in fig.6 and Fig.7. Spectrum analysis of u_{AC} waveform is reaching a value of Total Harmonic Distortion (THD) = 6%.

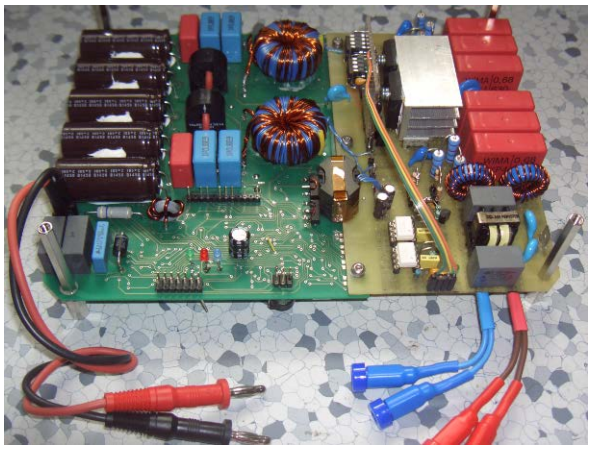

Figure 5. *An experimental prototype of active clamp DFBI inverter with SiC MOSFETs (P_{AC} = 200 W, peak efficiency 94%).*

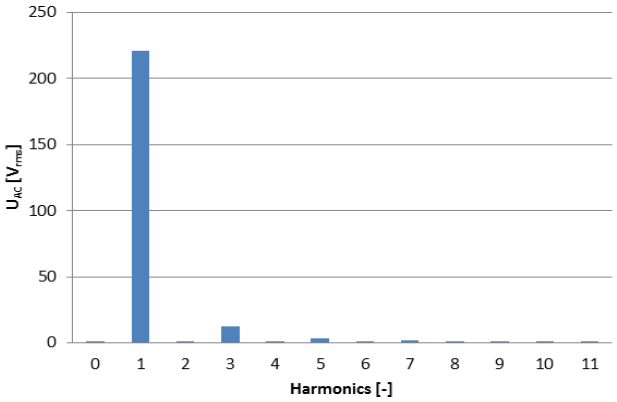

Figure 6. *Output voltage u_{AC} spectrum analysis (P_{AC} = 100W, U_{AC} = 230V, resistive load, THD = 6%).*

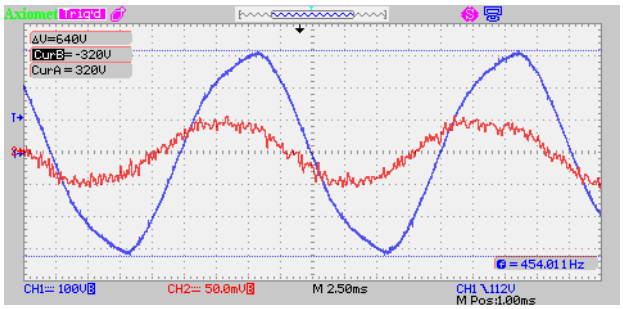

Figure 7. *Output voltage u_{AC} (blue) and output current i_{AC} (red), reactive power generation (U_{AC} = 230V, P_{AC} = 75W, S_{AC} = 81VA, serial R-C load, current probe 100mV/1A).*

The efficiency of DFBI was analyzed at three switching frequencies (48kHz, 67kHz, 100kHz). Those frequencies were chosen as the technical compromise between the size of energy storage components (fly-back transformer, resonant inductor L_r, output capacitors C_1 and C_2, active clamp capacitor C_C) and expected power losses (mainly in S_3 switch during reverse recovery of S_3 body diode). Fundamental switching frequency is below 150 kHz conducted EMC emissions minimum evaluation limit in this case.

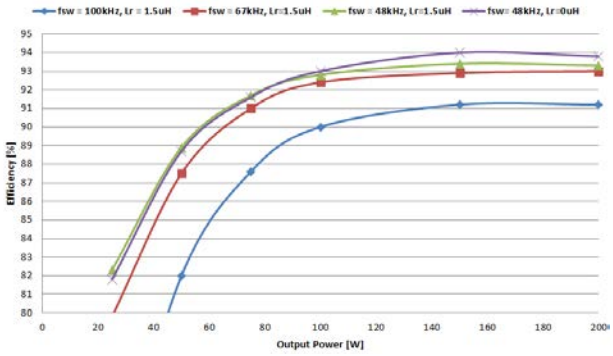

Figure 14. *Efficiency characteristics (U_{in} = 30V, U_{AC} = 230V).*

6 Conclusion

Modeling and experimental verification of steady-state operation of DFBI inverter using state-space analysis have been introduced in the paper. Besides, the efficiency of the DFBI inverter with SiC MOSFET C2M0280120D has been also provided. Peak efficiency 94% has been reached for this reduced component count power topology. Operation of DFBI in both active and reactive power generation mode has been presented as well. The benefit of this power topology is its relative simplicity and reactive power generation capability. The drawback of this power topology is the higher size of flyback transformers. Each of them needs to be dimensioned for 2*P_{AC} output power. This is the result of fly-back converters instantaneous power pulsation within output AC voltage time period. The efficiency of DFBI can be even more increased if the parallel combination of discrete SiC diode and SiC JFET transistor will be used on S_3 switch position.

6 Acknowledgement

The authors wish to thank to Slovak grant agency APVV for the project no. APVV-17-0218

Investigation of biological tissues with electromagnetic field interaction and its application in the development of new procedures in the design of electrosurgical instruments.

References:

[1] J. H. Lee, J. S. Lee and K. B. Lee, "Current sensorless MPPT method for a PV flyback microinverters using a dual-mode," *2014 International Power Electronics Conference (IPEC-Hiroshima 2014 - ECCE ASIA)*, Hiroshima, 2014, pp. 532-537.

[2] D. Hamza, M. Qiu and P. K. Jain, "Application and Stability Analysis of a Novel Digital Active EMI Filter Used in a Grid-Tied PV Microinverter Module," in *IEEE Transactions on Power Electronics*, vol. 28, no. 6, pp. 2867-2874, June 2013

[3] Abdalla, J. Corda and L. Zhang, "Multilevel DC-Link Inverter and Control Algorithm to Overcome the PV Partial Shading," in *IEEE Transactions on Power Electronics*, vol. 28, no. 1, pp. 14-18, Jan. 2013

[4] J. Steenis, K. Tsakalis and R. Ayyanar, "An Approach to Bumpless Control for LPV Modeled Inverters in a Microgrid," in *IEEE Transactions on Power Electronics*, vol. 29, no. 11, pp. 6214-6223, Nov. 2014.

[5] S. A. Khajehoddin, M. Karimi-Ghartemani, A. Bakhshai and P. Jain, "A Power Control Method With Simple Structure and Fast Dynamic Response for Single-Phase Grid-Connected DG Systems," in *IEEE Transactions on Power Electronics*, vol. 28, no. 1, pp. 221-233, Jan. 2013.

[6] C. N. M. Ho, H. Breuninger, S. Pettersson, G. Escobar and F. Canales, "A Comparative Performance Study of an Interleaved Boost Converter Using Commercial Si and SiC Diodes for PV Applications," in *IEEE Transactions on Power Electronics*, vol. 28, no. 1, pp. 289-299, Jan. 2013.

[7] E. Koutroulis and F. Blaabjerg, "Design Optimization of Transformerless Grid-Connected PV Inverters Including Reliability," in *IEEE Transactions on Power Electronics*, vol. 28, no. 1, pp. 325-335, Jan. 2013.

[8] S. Zengin, F. Deveci and M. Boztepe, "Decoupling Capacitor Selection in DCM Flyback PV Microinverters Considering Harmonic Distortion," in *IEEE Transactions on Power Electronics*, vol. 28, no. 2, pp. 816-825, Feb. 2013.

[9] H. Hu, S. Harb, N. Kutkut, I. Batarseh and Z. J. Shen, "A Review of Power Decoupling Techniques for Microinverters With Three Different Decoupling Capacitor Locations in PV Systems," in *IEEE Transactions on Power Electronics*, vol. 28, no. 6, pp. 2711-2726, June 2013.

[10] T. Suntio and A. Kuperman, "Comments on “An Efficient Partial Power Processing DC/DC Converter for Distributed PV Architectures”," in *IEEE Transactions on Power Electronics*, vol. 30, no. 4, pp. 2372-2372, April 2015.

[11] Xue, Y. Chang, L. Kjaer, Soeren B., BordonauJ., and T. Shimizu: Topologies of single-phase inverters for small distributed power generators: an overview. IEEE Trans. On Power Electronics, vol. 19, no. 5, p. 1305–1314, Sep. 2004.

[12] Papanikolaou, Nick P.: Low-voltage ride-through concept in fly-back inverter-based AC photovoltaic modules. *IET Power Electronics*, vol. 6, no. 7, p. 1436-1448, Aug. 2013.

[13] Beres, T., Dudrik, J., Eotvos, E.: Bidirectional step-up/step-down DC-DC converter for Hybrid Battery (in Slovak). *EE-Journal for Electrical Engineering and Electro-Energetics*, vol. 17, no. 1 (Feb. 2011), p. 31-32, ISSN 1335-2547.

[14] Frivaldsky, M., Dobrucky, B., Scelba, G., Spanik, P., Drgona, P.: Bidirectional step-up/step-down DC-DC converter with magnetically coupled coils. *Communication – Scientific Letters of the University of Zilina*, vol. 15, no. 3, p. 43-47.

[15] Dobrucky, B., Marcokova, M., Pokorny, M., Sul, R.: Using Orthogonal and Discrete Transform for Single-Phase PES Transients a New Approach. In *Proc. of IASTED-MIC’08 Int’l Conf. on Modeling, Iden-tification and Control*. Innsbruck (AT), Feb 2008, p. 440-445. ISBN 978-0-88986-712-3.

[16] Luo, F., Lin and Hong Y.E.: Energy Factor and Mathe-matical Modeling for Power DC/DC Converters. In *IEE Proc. on Electrical Power Application*, vol. 152, p. 191-198.

[17] Cernan, P., Dobrucky, B.: A Novel Control Algorithm of Dual Flyback Inverter Suitable for Dynamic and Nonlinear Loads. In *21st IASTED-MS’10 Int’l Conf. on Modelling and Simulation*, Banff, 2010, Paper no. 700-009.

[18] Dalal, D.: Design Considerations of Active Clamp and Reset Technique. *Application note No. SLUP 112*. Texas Instruments. 2001.